Smart Structures and Systems, *Vol. 19, No. 1 (2017) 47-56*
DOI: https://doi.org/10.12989/sss.2017.19.1.047

A wireless decentralized control experimental platform for vibration control of civil structures

Yan Yu[1], Luyu Li[*2], Xiaozhi Leng[1], Gangbing Song[3], Zhiqiang Liu[4] and Jinping Ou[2]

[1]*School of Electronic Science and Technology, Dalian University of Technology, Dalian, Liaoning, China*
[2]*School of Civil Engineering, Dalian University of Technology, Dalian, Liaoning, China*
[3]*Department of Mechanical Engineering, University of Houston, Houston TX, USA*
[4]*CCCC Highway Consultants Co., Ltd., Beijing 100088, P.R. China*

(Received May 9, 2016, Revised August 26, 2016, Accepted September 7, 2016)

Abstract. Considerable achievements in developing structural regulators as an important method for vibration control have been made over the last few decades. The use of large quantities of cables in traditional wired control systems to connect sensors, controllers, and actuators makes the structural regulators complicated and expensive. A wireless decentralized control experimental platform based on Wi-Fi unit is designed and implemented in this study. Centralized and decentralized control strategies as sample controllers are employed in this control system. An optimal control algorithm based on Kalman estimator is embedded in the dSPACE controller and the DSP controller. To examine the performance of this control scheme, a three-story steel structure is developed with active mass dampers installed on each floor as the wireless communication platform. Experimental results show that the wireless decentralized control exhibits good control performance and has various potential applications in industrial control systems. The proposed experimental system may become a benchmark platform for the validation of the corresponding wireless control algorithm.

Keywords: active mass damper; wireless decentralized control; benchmark; DSP; Wi-Fi

1. Introduction

With the development of building technology, more ultra-large buildings are being constructed around the world. As a result, the safety of civil structures, including buildings, bridges, dams, tunnels, and others, is of utmost importance. Structural vibration control technology uses passive or active devices to change structural properties such as damping, stiffness, mass, or the control force acting on the structure to achieve the response inhibition in the structure under external excitation (Xinfa, Zhenbin *et al*. 2014, Moon, Lim *et al*. 2007, Zhang, Zhou *et al*. 2013, Li, Marcassa *et al*. 2006). Generally, structure vibration control can be divided into four categories: (a) passive control (e.g., base isolation), (b) active control (e.g., active mass dampers), (c) semi-active control (e.g., semi-active variable dampers), and (d) hybrid control (Ou 2003). Active vibration control (AVC) requires a sensor or controller installation to measure the response of structures. In a traditional wired control scheme, cable installation can be time-consuming and costly (Dai 2010, Lynch, Wnag *et al*. 2008, Law, Swartz *et al*. 2009, Linderman and Spencer 2014, Yan *et al*. 2015). To eradicate the high cost of using cables, wireless systems could be a viable alternative. Wireless communication standards, such as Wi-Fi (IEEE 802.11b), have been developed, and reliable technologies have been widely adopted in many industrial applications (Feher 2011, Yan, Feng *et al*. 2016).

When the scale of the structure increases, centralized control systems with high instrumentation cost become difficult to reconfigure. These control systems could suffer from single-point failure at the controller. However, decentralized control strategies may solve these problems (Chen, Yu *et al*. 2010). Decentralized control was proposed in the 1970s to solve control problems of large-scale systems (Palacios Quinnoero, Rubio-Massegu *et al*. 2012, Davision, Aghdam *et al*. 2014, Yang 2007). At present, decentralized control systems are important in structural vibration control. Over the past few decades, studies have focused on decentralized control in structural engineering. For example, Sang-Myeong Kim conducted an experimental investigation of an active four-mount vibration isolation system and applied decentralized velocity feedback control (Zhao 2013). Yang, Swartz *et al*. (2007). examined a three-story, half-scale steel structure with magneto-rheological dampers installed on each floor and embedded closed-loop feedback control algorithms (Yang, Swartz *et al*. 2007). Interactions between dynamically coupled subsystems are considered as unknown disturbances, and each controller is designed as a single-input, single-output subsystem (Tong, Liu *et al*. 2011). These decentralized control algorithms account for the interconnections between subsystems as unknown disturbances; thus, each decentralized controller aims to improve local control performance, which does not generally result in global optimal control. If the controller

[*]Corresponding author, Professor
E-mail: liluyu @dlut.edu.cn

ISSN: 1738-1584 (Print), 1738-1991 (Online)

of a subsystem fails to operate properly during dynamic excitation, this subsystem may experience detrimental situations because neighboring subsystems focus on their own control performance and neglect the malfunctioning subsystem. In this decentralized control scheme, the controller of each subsystem requires local sensor data only, and each controller focuses on controlling the local subsystem. The block diagrams of centralized and decentralized controls are shown in Fig. 1.

The structure of this paper is as follows. Section 2 describes the sample control algorithms using LQG. The design of the wireless control system and experimental setup are presented in Sections 3 and 4, respectively. The experimental results of the proposed controllers based on WSNs are shown in Section 5. Finally, Section 6 concludes the paper.

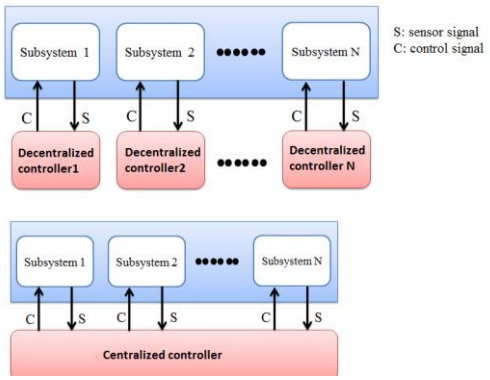

Fig. 1 Block diagram of decentralized control and centralized controls

2. Design of control algorithms

For a lumped-mass model with n degrees of freedom, the system motion equation of a controlled structural system can be formulated as

$$M\ddot{X}(t)+C\dot{X}(t)+KX(t)=T_u u(t)+T_w w(t) \quad (1)$$

where X(t) is the displacement vector relative to the shake table; M, C, K are the mass, damping, and stiffness matrices, respectively; w(t) and u(t) are the external excitation and control force vectors, respectively; and T_u and T_w are the control force and external excitation location matrices, respectively.

The state–space representation of the structural system can be written as

$$\dot{x} = Ax + Bu \quad (2)$$

where

$$x = [x_1(t), x_2(t), \cdots, x_n(t), \dot{x}_1(t), \dot{x}_2(t), \cdots, \dot{x}_n(t)]^T \quad (3)$$

$$A = \begin{bmatrix} 0 & I \\ -M^{-1}K & -M^{-1}C \end{bmatrix} \quad (4)$$

$$B = \begin{bmatrix} 0 \\ M^{-1}H \end{bmatrix} \quad (5)$$

The state–space vector x(t) can be related to the measurement vector y(t) as

$$y(t) = Cx(t) + Du(t) \quad (6)$$

where C and D are functions of the state variables selected to represent the measurements of the desired or available system. In this study, the relative displacements on all floors are measurable. However, the relative velocities cannot be quantified. Thus, C and D are expressed as

$$\begin{aligned} C &= [\text{eye}(3), \text{zeros}(3,3)] \\ D &= \text{zeros}(3,3) \end{aligned} \quad (7)$$

In this study, we assume a linear time invariant (LTI) system where stiffness, damping, and mass matrices do not change over time. Therefore, A, B, C, and D are assumed to be constant.

The linear quadratic regulator (LQR) based control design balances the good system response and required control effort (Lessard 2012). For the state–space representation of the structural control system defined in Eq. (2), assuming static measurement feedback, we compute the optimal feedback control force u(t) using a gain matrix K as

$$u(t) = -Kx(t) \quad (8)$$

where the gain matrix K is designed to minimize cost function J. The classical linear quadratic regulator (LQR) control minimizes a quadratic cost function J as follows

$$J(u)=\int_0^\infty (x^T(t)Q(t)x(t)+u^T(t)R(t)u(t))dt \quad (9)$$

where Q and R are two positive-definite Hermitian matrices.

The LQR control design assumes full-state feedback. However, full-state information is rarely available to the controller. Typically, only a few measurements are available, e.g., acceleration and displacement. Thus, an estimator is used to reconstruct the state elements used for the control law, as shown in Fig. 3. The Kalman filter is an optimal model-based, predictor–corrector type estimator that minimizes the variance of the estimated error covariance with a Gaussian-type process and measurement noise (Mohammadi and Plataniotis 2015, Qing, Karimi *et al*. 2015, Zhouxiong, Bo *et al*. 2015).

Kalman filters can be designed for each decentralized subsystem to estimate the global structural state using local sensor data. With available global state information, the controller is designed to optimize the overall system performance. The drawback of this control strategy is the estimation accuracy because of unavailable global sensor data. Although estimation can be improved by sharing (estimated or measured) information or control decisions, many issues have to be addressed to maximize the practical applications of these theoretical studies.

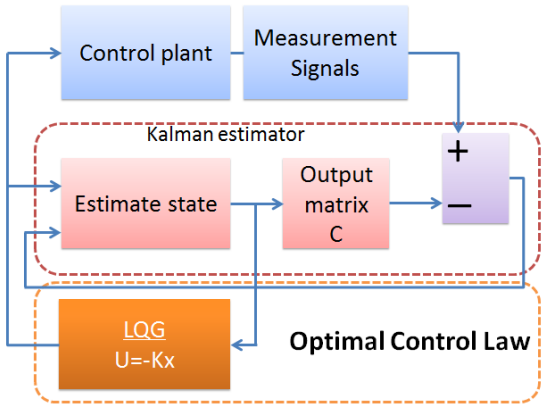

Fig. 2 Block diagram of control algorithm

In continuous time, the typical state–space plant model is represented as

$$\dot{x} = Ax + Bu + Gw$$
$$y = Cx + v \tag{10}$$

where w is the process noise and v is the measurement noise. The noise variables are assumed to be unrelated white noise processes with a covariance defined by

$$E(w)=E(v)=0, \quad E(ww^{T})=Q, \quad E(vv^{T})=R \tag{11}$$

An estimate of the state is obtained from the resulting estimator given by

$$\dot{\hat{x}}=A\hat{x}+Bu+L(y-C\hat{x}) \tag{12}$$

where the open-loop estimate accounting for system dynamics or time update is corrected using the measurement weighed by the Kalman gain, L, as shown in Fig. 3. If the estimated state is subtracted from the true state x, then the dynamics of the error in the estimate is represented by

$$\overline{x} = (A - LC)x \tag{13}$$

Eq. (10) becomes zero if the estimator gain is selected properly and the system is observable. Note that D is assumed to be zero because input does not directly feed through to the measurements in our applications.

The steady-state Kalman gain, L, is given by

$$L = PC^{T}R^{-1} \tag{14}$$

Similar to the LQR solution, error covariance P is the positive definite solution to the algebraic Riccati equation

$$AP + PA^{T} - PC^{T}R^{-1}CP + GQG^{T} = 0 \tag{15}$$

Matrices B and C are different for the centralized controller and decentralized one. Matrices B and C in the centralized controller represent three layers, and each matrix B and C in the decentralized controller represent only one layer. Thus, gain matrix K, L, and control force u(t) that was computed by gain matrix K also differ in the centralized controller and decentralized controller because of matrices B and C.

3. Wireless control system

3.1 Overall framework of wireless control system

In wired control systems, coaxial wires are used to provide communication links between sensors, actuators, and controllers. In this control system, sensors need to be deployed in the structure to collect structural response data during dynamic loading. Response data is fed into controllers to determine the required actuation forces and to apply control commands to the system actuators. As commanded by control signals, actuators employ control forces to mitigate undesirable structural responses. With the rapid development of wireless communication and embedded computing technologies, wireless sensing technology has expanded its applicability in active control systems to eliminate cables associated with traditional control systems (Yan, Jinhe *et al.* 2015).

In this study, wireless centralized and decentralized control systems are designed. The wireless control system is composed of the following parts: (1) wireless Wi-Fi sensing unit, (2) controller, (3) laser displacement sensor, (4) three-story steel model, and (5) shake table. In the two systems, three laser displacement sensors are used as sensors. The three-story steel model is the experimental model, and active mass dampers (AMDs) are considered as the actuators. In the wireless control system, the laser displacement sensors determine displacement after an initial state is given to the three-story steel model. A displacement signal is sent to the wireless transmission units. The wireless receiving units obtain the displacement signal that is sent to the three DSP controllers. The controllers calculate the optimal control force signal. The control signal is sent to the power amplifier that amplifies the signal to -6 V–6 V. The enlarged control signal acts on the actuator, which can effectively suppress the vibration of the three-story steel model. The decentralized control loop is shown in Fig. 3. The wireless centralized control system with the three-story steel model is illustrated in Fig. 4. The difference between the centralized control system and the decentralized control system is that the controllers are DSPs in the latter, whereas the controller is dSPACE in the former. The reason for such difference is that DSP is flexible and often used as the controller in the field of practical industrial application.

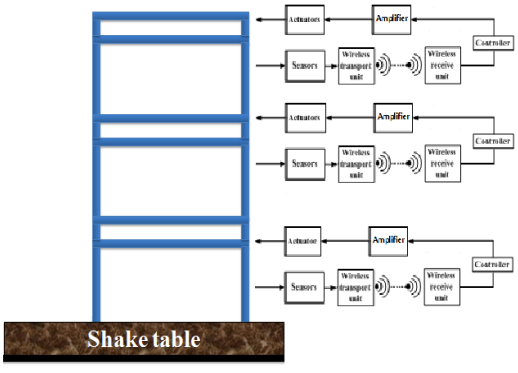

Fig. 3 Decentralized control loop

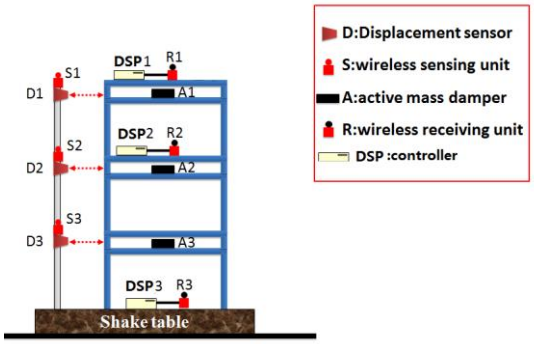

Fig. 4 Wireless decentralized control system

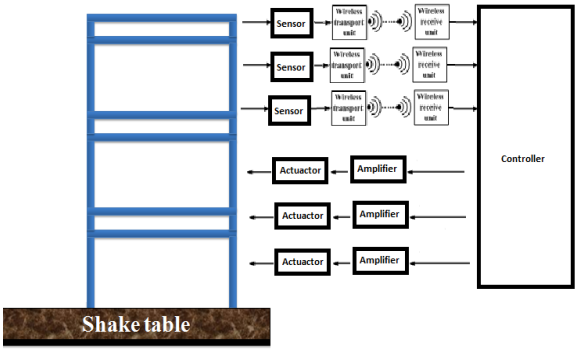

Fig. 5 Centralized control loop

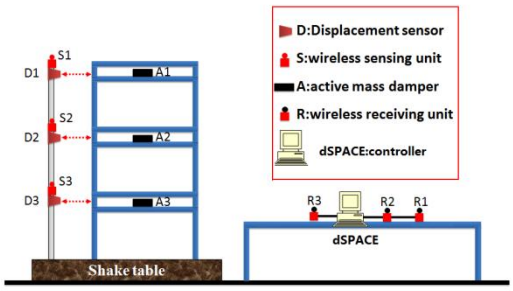

Fig. 6 Wireless centralized control system

Therefore, when the DSP controller is implemented, the control algorithm can be possibly used in practical applications. The decentralized control loop is shown in Fig. 5. The wireless centralized control system with the three-story steel model is illustrated in Fig. 6.

3.2 Hardware design of wireless sensing unit

As shown in Fig. 7, the wireless sensing unit consists of three functional modules: sensor signal digitization, computational core, and wireless communication. The sensing interface converts analog sensor signals into digital data that are transferred to the low-power, 16-bit MSP430F1612 microcontroller through a high-speed serial peripheral interface port. The microcontroller communicates with a wireless transceiver through a universal asynchronous receiver and transmitter interface. The Wi-Fi module operates in the 2.4 GHz international ISM (industrial, science, and medical) band, and all the hardware components are internally referenced at 5 V.

3.3 Hardware design of controllers

The centralized control program is mainly operated by dSPACE. The dSPACE real-time simulation system, which was developed by German company dSPACE, is a control system based on MATLAB/Simulink development. As a hardware-in-the-loop simulation software and hardware platform, the dSPACE real-time system based on rapid-control prototyping technology can perform offline and real-time simulation, modify the model design repeatedly to eliminate the errors in the early stage of design and consequently change the design minimizes costs. In this study, a dSPACE DS1104PPC controller board with rich I/O interface is used for centralized control.

In this design, three DSP F28335 processing units are used for decentralized controllers, and the model-based development method is employed to develop the distributed control algorithm software. To shorten the development cycle, a decentralized code is generated by TargetLink.

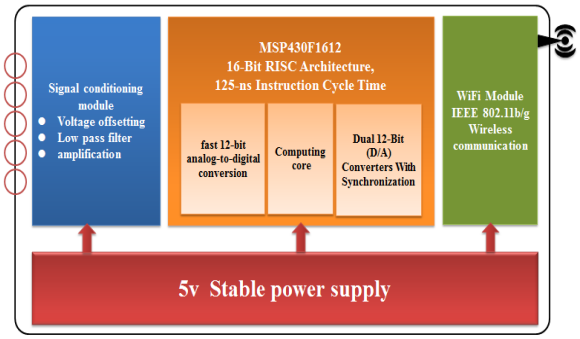

Fig. 7 Block diagram of wireless Wi-Fi sensing unit

Fig. 8 Hardware design of wireless sensing unit

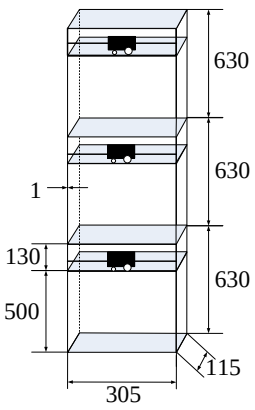

(a) Wind speed profile

(b) Wind direction profile

Fig. 9 Model parameters and physical map

Table 1 Details of model parameters

Component	Properties
Total dimensions	305 mm × 115 mm × 1890 mm
Dimensions of spring steel	1 mm × 115 mm × 500 mm
Mass of AMD	1.984 kg

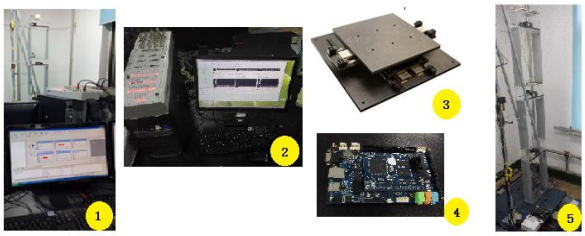

Fig. 10 ① Overall physical map of centralized control; ② dSPACE controller; ③shake table; ④ DSP controller; ⑤ Overall physical map of decentralized control

TargetLink is a software for automatic code generation that is based on a subset of Simulink/Stateflow models and produced by dSPACE GmbH. TargetLink requires an existing MATLAB/Simulink model to work on and generates both ANSI-C and production codes that are optimized for specific processors. This software also supports the generation of AUTOSAR-compliant code for automotive software components. Managing all relevant information for code generation occurs in a central data container called the data dictionary. Testing of the generated code is implemented in Simulink, which is also used for specifying underlying simulation models. TargetLink supports the following three simulation modes to test the generated code.

Model in the loop simulation (MIL): This mode allows the model design to be checked. An MIL simulation is also known as a floating-point simulation as because floating-point variables are typically used. Software in the loop (SIL): The simulation is based on the execution of generated code, which runs on a PC system with the plain or fixed-point variables typically used. Processor in the loop (PIL): In a PIL simulation, the generated code runs on the target hardware or an evaluation board. The so-called real-time frames are included. Thus, the simulation results as well as memory consumption and runtime information are transferred to the PC. In SIL, the C code is generated and placed in the simulation environment to check if the running results with and without C code are the same. MIL differs from SIL because the controller model in SIL is composed of the C code. PIL downloads the target code to the target processor. The generated code runs on an embedded processor, and the deviation between the MIL and SIL results is analyzed. The three previously mentioned modes of TargetLink are used to produce the control algorithm code for the DSP F28335. Thus, TargetLink significantly simplifies the testing process and improves the efficiency of software upgrading and updating.

The generated code is downloaded into DSP TMS320F28335 which is a high-precision processor with 32-bit floating-point processing units. The ADC result register is 16-bit, the digital quantity is in high 12 bits, and low 4 bits is invalid. Thus, the value in the ADC result should indicate a shift to the right 4 bits. TMS320F28335 kernel mainly includes the central processing unit (CPU), test units, and memory and peripheral interface units. The CPU is mainly composed of an arithmetic logic unit (ALU), multiplier, shifter, addressing, and operation units ARAU, and independent register. A CPU can completely access data and program memory and make address, shifting, decoding and executing instructions, arithmetic, and logic. The test logic unit is mainly used to monitor and control the operation of each part. The interface signal unit is the signal transmission channel between memory, peripherals, clock, CPU, and debug unit. As an editing tool for

TMS320F28335, CCS can provide environment configuration, program editing, compiling, linking, program debugging, tracking, and analyzing. In general, TMS320F28335 can accelerate the software development process and improve work efficiency using CCS.

4. Experimental setup

In this study, three AMDs were used to control the response of a three-story structure subject to shake table excitation. Wireless centralized and decentralized control strategies were implemented for comparison.

The experimental system used in this study on wireless structural control is a three-story spring-steel structure fitted with three AMD control systems on each floor. The structure comprises several components and has an overall height of 1.89 meters. Spring steel has a size of 1 mm x 115 mm and inter-story height of 500 mm. The mass of each AMD is 1.984 kg. A custom-direct current motor drives the AMD with the control force that is amplified by the power amplifier.

AMD is fitted with a DC motor. The input signal of the DC motor is the voltage one that was generated by the controller. Thus, AMD can move along with the expected trajectory. The shake table provides an external excitation signal for the three-story model. The controller calculates the control signals according to the measured displacement signal and the LQR control algorithm. With respect to the DC motor and in the range of rated power, an approximately linear relationship between torque and current, T=K*I, was observed. Coefficient K is called constant torque. The current signal follows the control system, and the current signal changes to a corresponding voltage one.

5. Experimental results and analysis

5.1 Preliminary validation experiments

To verify the effectiveness of the control scheme, the model of an initial state was presented and made into a free vibration. The experimental results are presented in Fig.s 11,12,13. In the following figures, the black dot line which is made up of dot represents the displacement result without control, the red stub line which is made up of stub represents the displacement result with wireless decentralized control and the blue full line represents the displacement result with wireless centralized control.

As shown by the experimental results, in an uncontrolled state, the model becomes stationary because of a vibration of approximately 110 s. In a control state, however, only 70 s is required to reach the stationary process. The introduction of control can significantly reduce the vibration amplitude in the model. Thus, the model quickly returns to a standstill. Experimental results indicate that the wireless control scheme that uses AMD is feasible and effective.

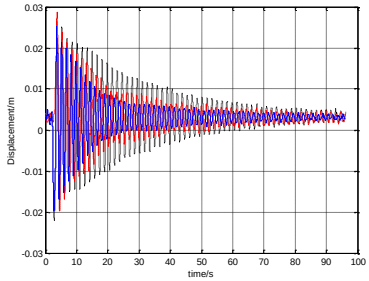

Fig. 11 Displacements of first layer under an initial state

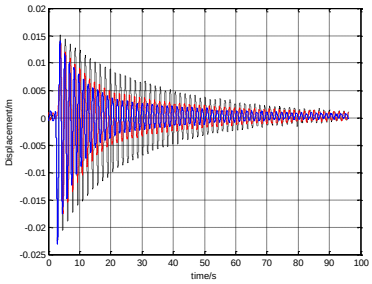

Fig. 12 Displacements of second layer under an initial state

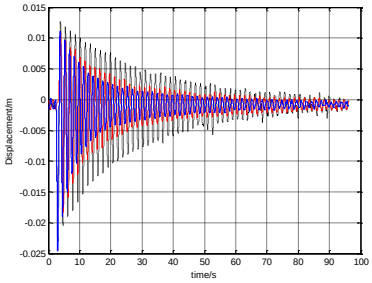

Fig. 13 Displacements of third layer under an initial state

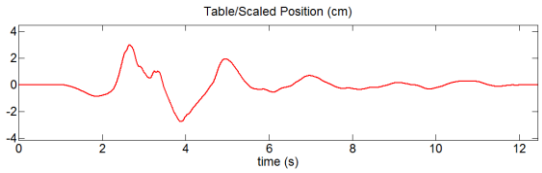

Fig. 14 Displacement of shake table under EI excitation

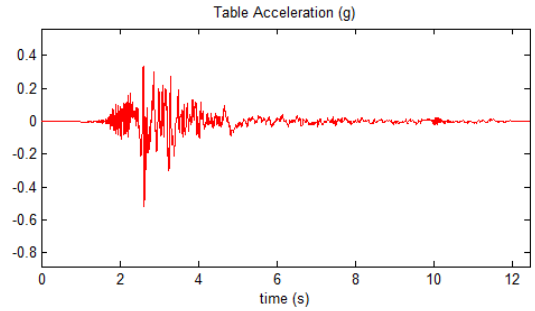

Fig. 15 Acceleration of shake table under EI excitation

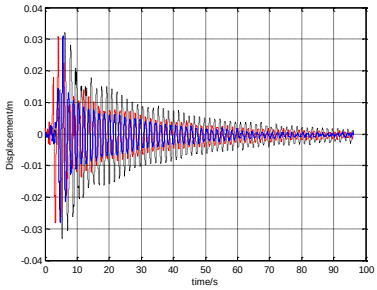

Fig. 16 A Displacements of first layer under EI excitation

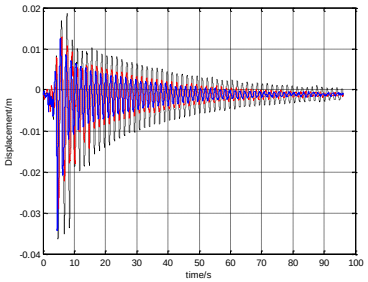

Fig. 17 Displacements of second layer under EI excitation

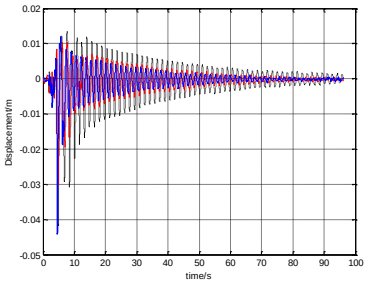

Fig. 18 Displacements of third layer under EI excitation

5.2 Seismic excitation situations

To accurately verify the general applicability of this method, the three-story model was given the seismic signals that were generated by the shaking table. The model obtains control performance by the displacement sensors. The experimental results are shown in the succeeding figures.

5.2.1 EI seismic excitation signal

5.2.2 Kobe seismic excitation signal

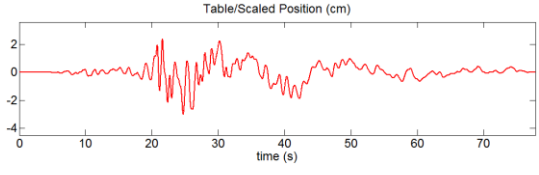

Fig. 19 Displacement of shake table under Kobe excitation

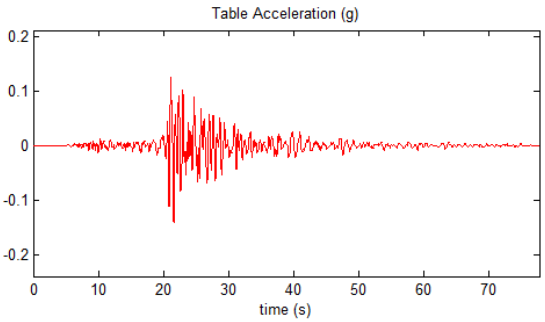

Fig. 20 Acceleration of shake table under Kobe excitation

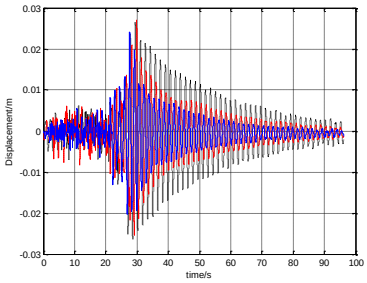

Fig. 21 Displacements of first layer under Kobe excitation

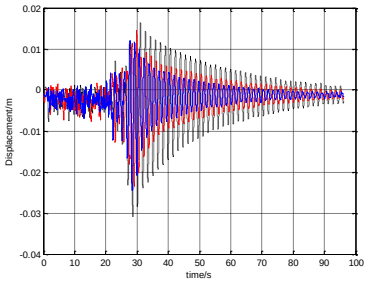

Fig. 22 Displacements of second layer under Kobe excitation

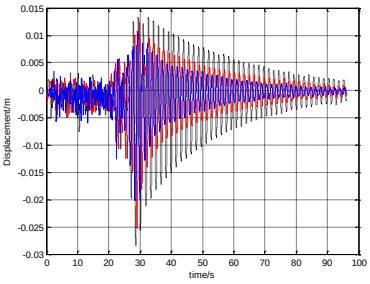

Fig. 23 Displacements of third layer under Kobe excitation

5.2.3 Cape seismic excitation signal

5.2.4 Northridge seismic excitation signal

In the wireless control system, the control voltage signal increases with the displacement of the model increases

when the voltage is large enough to drive the DC motor. The motor rotates to facilitate the movement of the active mass damper. Initially, the voltage signal generated by the controller is insufficient to drive the DC motor because the displacement model is extremely small. Thus, both centralized and decentralized controls do not work. As a result, the waveforms of the centralized and decentralized controls are mainly consistent with that without control waveform. As displacement increases when the voltage signal is high enough to drive the motor, AMD is important in suppressing the vibration of the structure. Ultimately, the motor stops because the displacement is too small. The control effect is most evident before and after the maximum displacement.

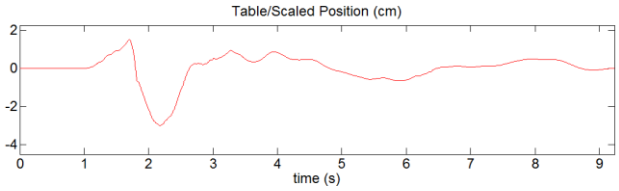

Fig. 24 Displacement of shake table under Cape excitation

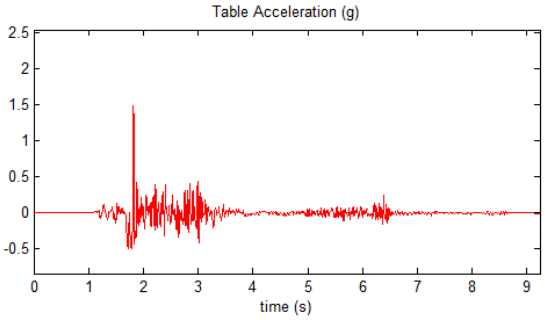

Fig. 25 Acceleration of shake table under Cape excitation

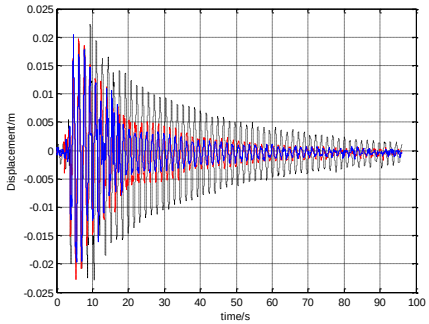

Fig. 26 Displacements of first layer under Cape excitation

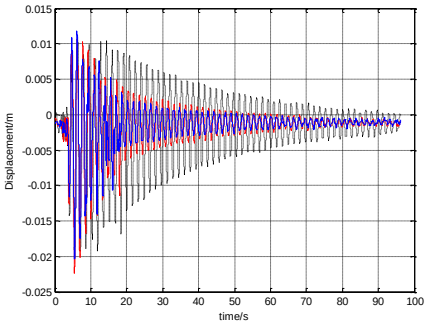

Fig. 27 Displacements of second layer under Cape excitation

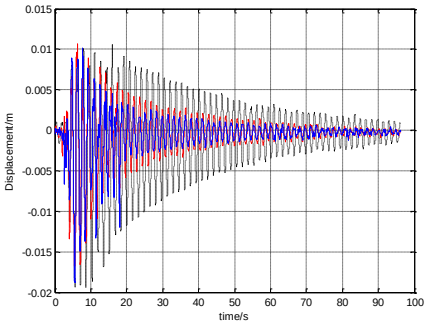

Fig. 28 Displacements of third layer under Cape excitation

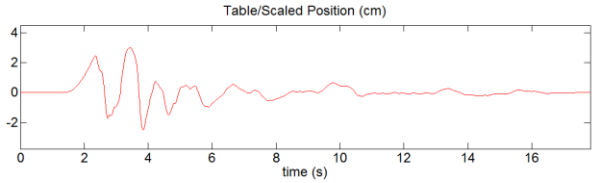

Fig. 29 Displacement of shake table under Northbridge

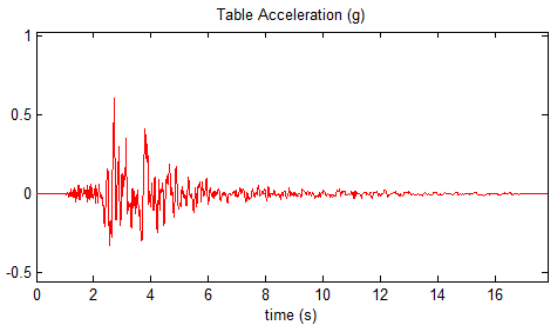

Fig. 30 Acceleration of shake table under Northbridge

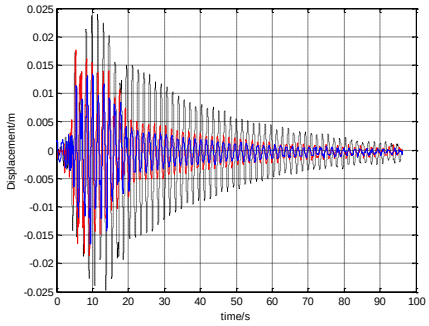

Fig. 31 Displacements of first layer under Northbridge

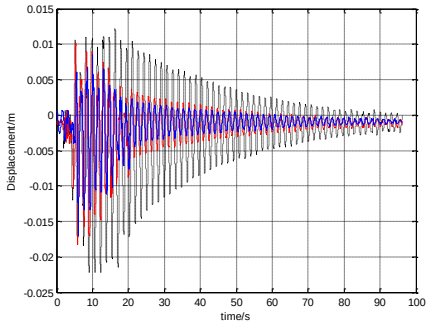

Fig. 32 Displacements of second layer under Northbridge

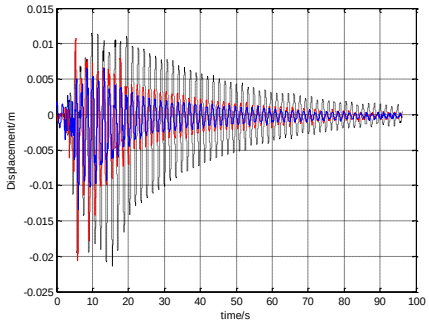

Fig. 33 Displacements of third layer under Northbridge

As indicated by the experimental results, both the centralized and decentralized controls exhibit good control performance. However, the control performance of the decentralized control is slightly worse than that of the centralized control. It is caused by time synchronization and the optimal gain matrix. In the decentralized control scheme, the input signal of the system is only the displacement of the current layer. However, in the centralized control system, the optimal control matrix is calculated according to the displacement of all the three layers. In the decentralized control system, time synchronization affects control, which can be ignored in the centralized control system.

5. Conclusions

In this paper, a wireless decentralized control experimental platform for structural vibration control was developed based on Wi-Fi unit. Based on optimal control and Kalman estimator theory, the sample controllers which are centralized control and distributed control were implemented. The experimental results showed the feasibility of the proposed wireless decentralized control experimental platform. Moreover, the decentralized control can significantly improve the fault tolerance of the system compared with the centralized control. On the other hand, time synchronization and coupling between the layers in the decentralized control system are two serious problems that will be addressed in the next stage of our study.

Acknowledgments

This work was supported by the National Natural Science Foundation of China (Project No. 51678108, 51378093, 51161120359), International S&T Cooperation Program of China (2015DFG82080), the Fundamental Research Funds for the Central Universities (Grant No. DUT15ZD117), Program for Liaoning Excellent Talents in University (LJQ2015028), and the National Basic Research Program of China (Grant No. 2011CB013705). We express our sincere thanks.

References

Chen, J., Cao, X., Cheng, P., Xiao, Y. and Sun, Y. (2010), "Distributed collaborative control for industrial automation with wireless sensor and actuator networks", *IEEE T. Ind. Electron.*, **57**(12), 4219-4230.

Chen, J., Yu, Q., Zhang, Y., Chen, H. and Sun, Y. (2010), "Feedback based clock synchronization in wireless sensor networks: A control theoretic approach", *IEEE T. Vehicular Technol.*, **59**(6), 2963-2973.

Dai J. (2010), "Simulation study on the hierarchical decentralized control of structural vibration", *Proceedings of the IEEE 2nd International Conference on Computer Modeling and Simulation, ICCMS'10.*

Davison, E.J. and Aghdam, A.G. (2014), "Decentralized control of large-scale systems", *Springer Publishing Company, Incorporated.*

Feher, K. (2011), "Remote control, cellular, WiFi, WiLAN, mobile communication and position finder systems", *U.S. Patent* No. 7,904,041.

Law, K.H., Lynch, J. and Wang, Y. (2008), "Wireless sensing and structural control strategies", *Proceedings of the 4th International Workshop on Advanced Smart Materials and Smart Structures Technologies (ANCRiSST).*

Law, K.H., Lynch, J. and Wang, Y. (2009), "Decentralized control strategies with wireless sensing and actuation", *Proceedings of the 2009 NFS CMMI Engineering Research and Innovation Conference, Honolulu, Hawaii*.

Lessard, L. (2012), "Decentralized LQG control of systems with a broadcast architecture", *IEEE Conference on Decision and Control.*

Li, Y., Marcassa, F., Horowitz, R., Oboe, R. and Evans, R. (2006), "Track-following control with active vibration damping of a PZT-actuated suspension dual-stage servo system", *J. Dynam.*

Syst. Meas. Control, **128**(3), 568-576.
Linderman, L.E. and Spencer, B.F. (2014), "Smart wireless control of civil structures", *Newmark Structural Engineering Laboratory, University of Illinois at Urbana-Champaign*.
Lynch, J.P., Wang, Y., Swartz, R.A., Lu, K.C. and Loh, C.H. (2008), "Implementation of a closed-loop structural control system using wireless sensor networks", *Struct. Control Health Monit*., **15**(4), 518-539.
Mohammadi, A. and Plataniotis, K.N. (2015), "Structure-induced complex Kalman filter for decentralized sequential Bayesian estimation", *IEEE Signal Pr. Lett.*, **22**(9), 1419-1423.
Moon, S.J., Lim, C.W., Kim, B.H and Park, Y. (2007), "Structural vibration control using linear magnetostrictive actuators", *J. Sound Vib*., **302**(4-5), 875-891.
Ou, J.P. (2003), "Structural vibration control-active, semi-active and smart contro", *Science, China*.
Palacios-Quinonero, F., Rubio-Massegu, J., Rossell, J.M. and Reza Karimi, H. (2012), "Discrete-time static output-feedback semi-decentralized H∞ controller design: an application to structural vibration control", *Proceedings of the American Control Conference (ACC), 2012. IEEE*.
Qing, X., Karimi, H.R., Niu, Y. and Wng, X. (2015), "Decentralized unscented Kalman filter based on a consensus algorithm for multi-area dynamic state estimation in power systems", *Int. J. Elec. Power Energy Syst*., 65, 26-33.
Sun, Z., Li, B., Dyke1, S.J. and Liu, C. (2015), "Benchmark problem in active structural control with wireless sensor network", *Struct. Control Health Monit*., **23**(1), 20-34.
Tong, S., Liu, C., Li, Y. and Zhang, H. (2011), "Adaptive fuzzy decentralized control for large-scale nonlinear systems with time-varying delays and unknown high-frequency gain sign", *Systems, Man, Cybernetics, Part B: Cybernetics, IEEE*, **41**(2), 474-485.
Wang, Y., Swarts, R.A., Lynch, J.P. and Kaw, K.H. (2007), "Decentralized civil structural control using real-time wireless sensing and embedded computing", *Smart Struct. Syst*., **3**(3), 321-340.
Xinfa, Z., Zhenbin, P., Lian-Guang, M. and Yu, S. (2014), "Active control based on prediction of structural vibration feedback", *Proceedings of the IEEE 2014 5th International Conference on Intelligent Systems Design and Engineering Applications (ISDEA)*.
Yang, X., Hongxing, H. and Junwei, H. (2007), "Three state controller design of shaking table in active structural control system", *Proceedings of the IEEE International Conference on Control and Automation, ICCA 2007*.
Yu, Y., Guo, J., Li, L., Song, G. and Li, P. (2015), "Experimental study of wireless structural vibration control considering different time delays", *Smart Mater. Struct*., 24045005.
Yu, Y., Han, F., Bao, Y., Ou, J. (2016), "A study on data loss compensation of wi-fi-based wireless sensor networks for structural health monitoring", *IEEE Sensors J*., **16**(10), 3811-3818
Yu, Y., Han, F., Leng, X., Li, L., Guo, J. and Ou, J. (2015), "Design and implementation of a wireless optimal control scheme for active structural vibration control", *Proceedings of the 5th International Conference on Instrumentation and Measurement, Computer, Communication and Control(IEEE IMCCC 2015)*, September 18-20, Qinghuangdao.
Zhang, Q., Zhou, L., Zhang, J. and Jin, J. (2013), "Efficient modal control for vibration suppression of a flexible parallel manipulator", *Proceedings of the 2013 IEEE International Conference on Robotics and Biomimetics (ROBIO)*.
Zhang, Z., Wang, Z., Wang, Y.C. and Zhang, H. (2013), "Multi-overlapping decentralized control of a class of structural vibration systems", *Proceedings of the 2013 32nd Chinese Control Conference (CCC), IEEE*.

BS